Advances in Applied Energy 10 (2023) 100139

Contents lists available at ScienceDirect

Advances in Applied Energy

journal homepage: www.elsevier.com/locate/adapen

Decarbonizing all-electric communities via carbon-responsive control of behind-the-meter resources

Jing Wang, Rawad El Kontar, Xin Jin*, Jennifer King

National Renewable Energy Laboratory, 15013 Denver West Parkway, Golden, CO 80401, United States

ARTICLE INFO

Keywords:
Decarbonization
Electrification
Control
Electric vehicle charging
HVAC
All-electric community

ABSTRACT

The progression of electrification in the building and transportation sectors brings new opportunities for energy decarbonization. With higher dependence on the grid power supply, the variation of the grid carbon emission intensity can be utilized to reduce the carbon emissions from the two sectors. Existing coordinated control methods for buildings with distributed energy resources (DERs) either consider electricity price or renewable energy generation as the input signal, or adopt optimization in the decision-making, which is difficult to implement in the real-world environment. This paper aims to propose and validate an easy-to-deploy rule-based carbon responsive control framework that facilitates coordination between all-electric buildings and electric vehicles (EVs). The signals of the grid carbon emission intensity and the local photovoltaics (PV) generation are used for shifting the controllable loads. Extensive simulations were conducted using a model of an all-electric mixed-use community in a cold climate to validate the control performance with metrics such as emissions, energy consumption, peak demand, and EV end-of-day state-of-charge (SOC). Our study identifies that 4.5% to 27.1% of annual emission reduction can be achieved with limited impact on energy costs, peak demand, and thermal comfort. Additionally, up to 32.7% of EV emission reduction can be obtained if the EV owners reduce the target SOC by less than 21.2%.

1. Introduction

To combat climate change, research and technologies for decarbonization are advancing rapidly all over the globe. In the United States, the building and transportation sectors together accounted for 72% of the total energy-related carbon dioxide (CO_2) emissions in 2021 [1]. Electrification in these two sectors provides new opportunities for reducing carbon emissions. For instance, state and municipal building codes in the United States [2] are beginning to require buildings to become all-electric. Moreover, electric vehicle (EV) penetration rates are rising globally—nearly 10% of all cars sold worldwide in 2021 were electric [3].

Given the persistent electrification of new buildings and vehicles, a higher dependence on the power grid is expected from the transportation and building sectors. Further, due to lasting changes in the grid power generation mix, the grid carbon emission intensity is fluctuating. Therefore, there is great potential to utilize time-varying grid carbon emission intensity in building and EV load control. More specifically, shifting building and EV charging loads from higher-intensity hours to cleaner hours in response to grid carbon intensity signals can reduce carbon emissions and thus help achieve decarbonization goals.

Existing research on emission reduction-driven control for buildings or EVs is primarily focused on optimization-based methods, where optimization techniques are used to design control strategies that achieve desired system behavior while minimizing selected performance metrics. Leerbeck et al. [4] developed a model predictive control (MPC) based heat pump controller for building space heating. The control inputs include weather and CO_2 emission forecasts. Results showed that approximately 16% of CO_2 emission reduction was achieved in well-insulated new buildings with floor heating systems. Gasser et al. [5] studied building flexibility using MPC, where air-source heat pumps for space heating and EVs were involved as controllable loads. When carbon emissions were considered in the objective function, up to 21% of emissions were reduced compared to the baseline. Dixon et al. [6] investigated coordinated charging of EVs to reduce CO_2 emissions while absorbing excess wind generation. It was found that the average emissions rate of 35–56 gCO_2/km from traditional EV charging can be reduced to 28–40 gCO_2/km by controlled charging.

Some studies adopt reinforcement learning (RL) techniques in emission reduction related building control. Jeen et al. [7] proposed a probabilistic emission-abating RL algorithm, which only requires a short period of active training and does not need building-specific simulators or data a priori. In their experiments across three varied building energy simulations, the proposed RL algorithm outperformed an existing rule-based controller and other popular RL baselines by as much as 31% in terms of building emissions.

* Corresponding author.
E-mail address: xin.jin@nrel.gov (X. Jin).

https://doi.org/10.1016/j.adapen.2023.100139
Received 20 February 2023; Received in revised form 8 April 2023; Accepted 19 April 2023
Available online 22 April 2023

Table 1
Summary of literature on building and EV emission reduction-driven control, revealing a focus on single buildings in building studies and larger scales in EV studies. The literature shows a lack of rule-based coordination at the community-scale level for buildings and EVs.

Reference	Objective	Scale	Control method	Controlled system	DERs
[4]	Emission reduction	Building (house, office)	MPC	HVAC	None
[5]	Emission and cost reduction, flexibility	Building (multifamily)	MPC	HVAC, DHW, TES, EV	PV, TES
[12]	Emission and cost reduction, thermal energy	Building (apartment)	MPC	HVAC, DHW	TES
[13]	Emission reduction	Grid	Optimization	EV	N/A
[6]	Emission reduction, less wind curtailment	Grid	Optimization	EV	Wind
[14]	Emission reduction	Traffic analysis zone	Optimization	EV	N/A
[7]	Emission reduction	Building (mixed-use, office, seminar center)	RL	HVAC	None
[9]	Emission, cost, and peak load reduction	Building (residential)	Rule-based	HVAC, DHW	TES
[10]	Emission reduction	Community (residential)	Rule-based	HVAC, DHW, battery	PV, battery, TES
[11]	Emission reduction	Community (mixed-use)	Rule-based	EV	None
Proposed work	Emission reduction	Community (mixed-use)	Rule-based	HVAC, EV, battery	PV, battery, TES

Despite the advancement of optimization-based building and EV controllers in research, rule-based controllers are still the dominant controllers used in most real-world applications in buildings and EV chargers. This type of control strategy design typically involves defining a set of rules or logical statements to determine the appropriate control actions for a given system state. When carefully designed, some rule-based controllers perform comparably to optimization-based ones and become good alternatives [8]. Clauß [9] studied predictive rule-based control for reducing the CO_2 equivalent greenhouse gas emissions ($CO_{2eq.}$). The heat pump system for a Norwegian single-family detached house was controlled with historical weather and $CO_{2eq.}$ emission data from 2015 as inputs. They identified limited annual $CO_{2eq.}$ emission reductions due to small daily fluctuations in the Norwegian electricity grid $CO_{2eq.}$ intensities. In the authors' previous publications, rule-based carbon responsive control frameworks were designed and applied to building heat pump systems [10] and EV charging loads [11], respectively. Up to 20.5% of annual household carbon emissions and 12.7% of EV charging emissions were achieved through the proposed control algorithms.

Table 1 summarizes relevant literature on emission reduction-driven control work for buildings and EVs. From the table, we see that most building emission control studies focus on single buildings, while EV related emission control considers a much larger scale, such as the grid or traffic analysis zone. As previously mentioned, optimization is still the dominant control method for emission reduction-driven control in the literature. Here, "optimization" refers to unspecified optimization methods other than MPC and RL. Heating, ventilating, and air-conditioning (HVAC) systems and domestic hot water (DHW) systems are the most common controlled systems in building emission control work. In terms of distributed energy resources (DERs), some studies involve renewable energy generation such as photovoltaics (PV) and wind. Temporal arbitrage such as electric batteries and thermal energy storage (TES) are also considered in some cases. Here, TES mainly refers to the hot water tanks in building DHW systems. Note that unless listed in the "controlled system" column, the DERs here are not necessarily controlled. Based on the literature review, there is a lack of rule-based community-scale coordination of buildings and EVs in the current state of the art of emission reduction control.

In this work, we propose a rule-based control algorithm for coordinating building loads and EV charging loads to decarbonize energy use, with the presence of PV generation and batteries. Note that because we focus on the operational stage of buildings, embodied carbon emissions are not within the discussion scope of this work. Forecasts of the grid carbon emission intensity are used as inputs for decision-making, where we assume the input data are perfect forecasts. The control algorithm has been validated on the model of an all-electric, mixed-use community being constructed in Denver, Colorado, United States. Through the simulation case study, the impact of the emission reduction control algorithm on energy use, costs, peak demand, thermal comfort, and DER performances will be discussed. This work aims to answer the following research questions:

- How should we coordinate building loads with EV charging loads to reduce operational carbon emissions through rule-based control?
- What extra considerations need to take place if DERs such as PV and batteries are present?
- How does such emission reduction control affect energy use and costs, peak demand, and occupant thermal comfort?

The remainder of this paper is organized as follows: Section 2 presents the overall workflow and the research methodology of the proposed emission reduction control framework. Section 3 describes the case study community and the simulation inputs for the case study. Section 4 discusses the simulation results with various metrics such as emissions, energy, cost, and thermal comfort along with a sensitivity analysis. Section 5 concludes the work and recommends future topics for further study.

2. Methodology

The overall workflow of this paper is shown in Fig. 1. The community building energy models with EV loads are first built in the URBANopt™ [15,16] modeling platform. In this community model, the buildings are adapted from DOE prototypical building model 90.1-2009 templates, which were developed to reflect the energy efficiency requirements of the ASHRAE Standard 90.1-2009 [17] in commercial buildings. The EV loads are pre-generated EV charging profiles from EVI-Pro [18,19]. Details about the modeling of the community can be found in reference [20]. Based on the community energy model, REopt™ [21] is then used to optimally size the DERs. Using the annual building energy profiles simulated from Step 1, REopt optimizes the PV and battery sizes with mixed-integer linear programming based on assumptions about PV energy production, battery characteristics, equipment costs, financing options, and incentives and tax credits, etc. It is noted that the PV sizes in this work were designed to meet annual net zero energy goals at each building level.

Following Step 2, the control algorithms are then implemented with OpenStudio™ measures and integrated into the URBANopt workflow. Two different control measures, namely the baseline control and the coordinated control are implemented separately. The detailed control algorithms will be introduced in the following subsections. Finally, annual energy simulations are conducted and the results for the coordinated control scenario are evaluated using selected metrics against the baseline scenario.

2.1. Coordinated control

The proposed coordinated control algorithm coordinates the building HVAC system, EV charging, and battery charging/discharging for operational carbon emission reduction based on inputs of grid carbon intensities and local PV generation. The flowchart in Fig. 2 visualizes the decision-making process of the proposed rule-based controller, which repeats daily. Conceptually, it can be divided into net-load determination,

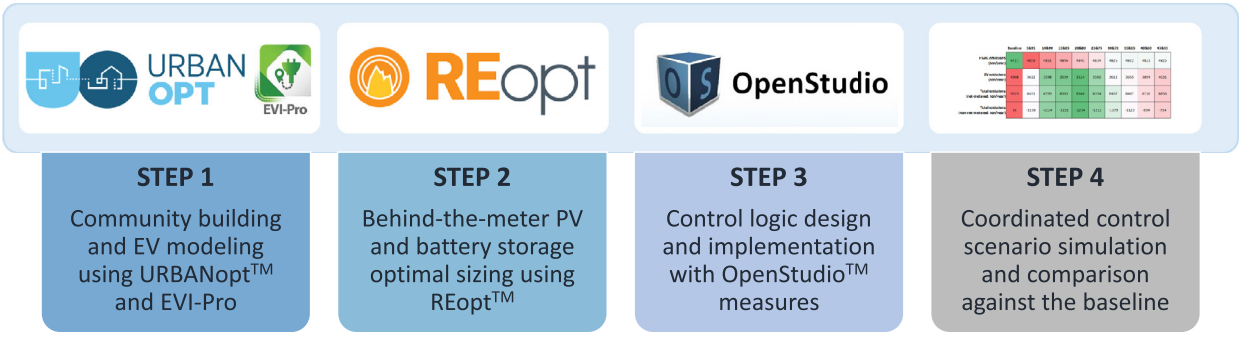

Fig. 1. The workflow of this paper, which involves building community energy models with EV loads in URBANopt and optimizing the DERs using REopt. OpenStudio measures are then used to implement control algorithms, and annual energy simulations are conducted to evaluate the results of the coordinated control scenario against the baseline scenario.

emission reduction control rules, HVAC and EV control, battery control, and grid power calculation.

The interconnection between each part of the control logic is described as follows. Depending on whether the building uses electricity from the grid, the controller will adopt different strategies. If the building is using grid electricity (i.e., net-load is positive), emission reduction control rules will be implemented, adjusting the zone HVAC setpoints and EV charging loads according to the grid's carbon intensity. The battery will only discharge when using grid electricity, and only if the grid carbon intensity is high. On the other hand, if PV power generation can cover the total building load (i.e., net-load is negative), the building will consume PV energy first. In this case, the controller will adopt the same control actions as it does when the grid power is clean. Additionally in this case, the battery will be charged using local PV energy after the building loads are satisfied. The details for each part of the control are described in the remainder of this subsection.

Net-load determination To determine whether the building is using the electricity from the grid or the locally generated PV energy, the net-load needs to be calculated by subtracting the PV generation from the total building load. Because the building load at the current timestep is not known before making the control decisions, here we use the load from the last timestep for estimating the net-load ($P^{t-1}_{load} - P^{t}_{pv}$). If positive, it means the building is using the grid electricity, and the carbon emission reduction control mechanism kicks in. Conversely, if negative, clean local PV energy is used, and we increase the HVAC and EV loads to enable load shifting to cleaner hours. This could also potentially increase the PV self-consumption rate. Here we note that using the building load from the last timestep in the net-load calculation might lead to a discrepancy between the predicted and actual net-load. This, in some cases, will further lead to a frequent change of the sign of the net-load, and thus result in controlled load fluctuations. Enlarging the control timestep as we did in this paper or having a feedback loop can mitigate the problem.

Based on the authors' earlier study [10] where various emission reduction controllers were compared, enabling carbon net-metering will result in better control performance such as lower carbon emissions. Therefore, we introduce both energy and carbon net-metering in this work. This means for the PV energy exported back to the grid, the prosumer will obtain both energy and emission credits to offset its total energy usage and carbon emissions.

Emission reduction control rules The emission reduction control takes effect when the building net-load is positive. It shifts the controllable loads (i.e., HVAC and EV) to hours with lower carbon emission intensities based on the grid emission signals. To accomplish this, a common method is to divide the carbon intensity data range into several regions, where each region correlates with one type of control action [9]. In this paper, we divide the carbon emission data range into three regions with two thresholds, the higher threshold (HT) and the lower threshold (LT). Between the two thresholds, default HVAC system setpoints $T_{set,default}$ and moderate EV load shifting will be implemented. When above the HT, less HVAC and EV loads will occur, and vice versa. The values of the HT and LT are carefully selected through a sensitivity analysis introduced in Section 4.1.

HVAC and EV control The HVAC system is controlled through zone thermostat setpoint control. The default setpoints $T_{set,default}$ are the same as those in the baseline. Below the LT, which is the clean zone, the $T_{set,clean}$ will be implemented, and vice versa. To maintain occupant thermal comfort, we designed the $T_{set,clean}$ to be 1 °C lower than the $T_{set,default}$ for space cooling and 1 °C higher for space heating. For $T_{set,unclean}$, it is 1 °C above the $T_{set,default}$ for cooling and 1°C below for heating. The clean setpoints $T_{set,clean}$ are also adopted when the building net-load is negative and PV energy is used.

The EV charging control adjusts the charging power P^{t}_{ev} through a similar algorithm. Because the EV loads in this work are modeled as pre-generated accumulated load profiles for each building instead of arrival and departure events for each individual EV, we used the original EV load profiles as the baseline and shifted the loads based on them. For the unclean hours (i.e., intensity higher than HT), zero EV charging power is dictated. We note that in the real world, standards will require a minimum non-zero charging power to keep the charging process active. The zero EV charging power here is assumed for simplification. For the hour that lies between the HT and LT, EV power is calculated using the following equation:

$$P^{t}_{ev} = (1 - \frac{e^{t} - LT}{HT - LT}) * P^{t}_{orig}, \tag{1}$$

where P^{t}_{orig} is the originally scheduled EV power in the baseline. The e^{t} represents the grid emission intensity at the current timestep t, which lies in between LT and HT. Therefore, this equation ensures that when the carbon intensity is larger than LT, EV load will be curtailed. The closer it is to HT (i.e., unclean), the smaller the EV power.

For the clean hours (i.e., intensity lower than LT or net-load negative), a load compensation for the accumulated curtailed EV energy for the day will be implemented. The power for curtailment compensation is calculated by:

$$P^{t}_{ev} = P^{t}_{orig} + \frac{E^{t}_{curt}}{\Delta t}, \tag{2}$$

where E^{t}_{curt} is the accumulated curtailed EV energy for the day until the current timestep; Δt is the control timestep. During the compensation, the effective EV power P^{t}_{ev} is larger than the original power P^{t}_{orig}. In this way, the EV load is shifted from the unclean hours to the clean hours. To mitigate the potential peak demand increase issue due to EV load shifting, an upper limit for P^{t}_{ev} is set as the maximum charging power of the EV charger, which varies with the building size. Additionally, when the compensation is using PV energy, the effective EV load cannot be greater than the absolute net-load value ($P^{t}_{pv} - P^{t-1}_{load}$) to avoid flipping signs of the net-load.

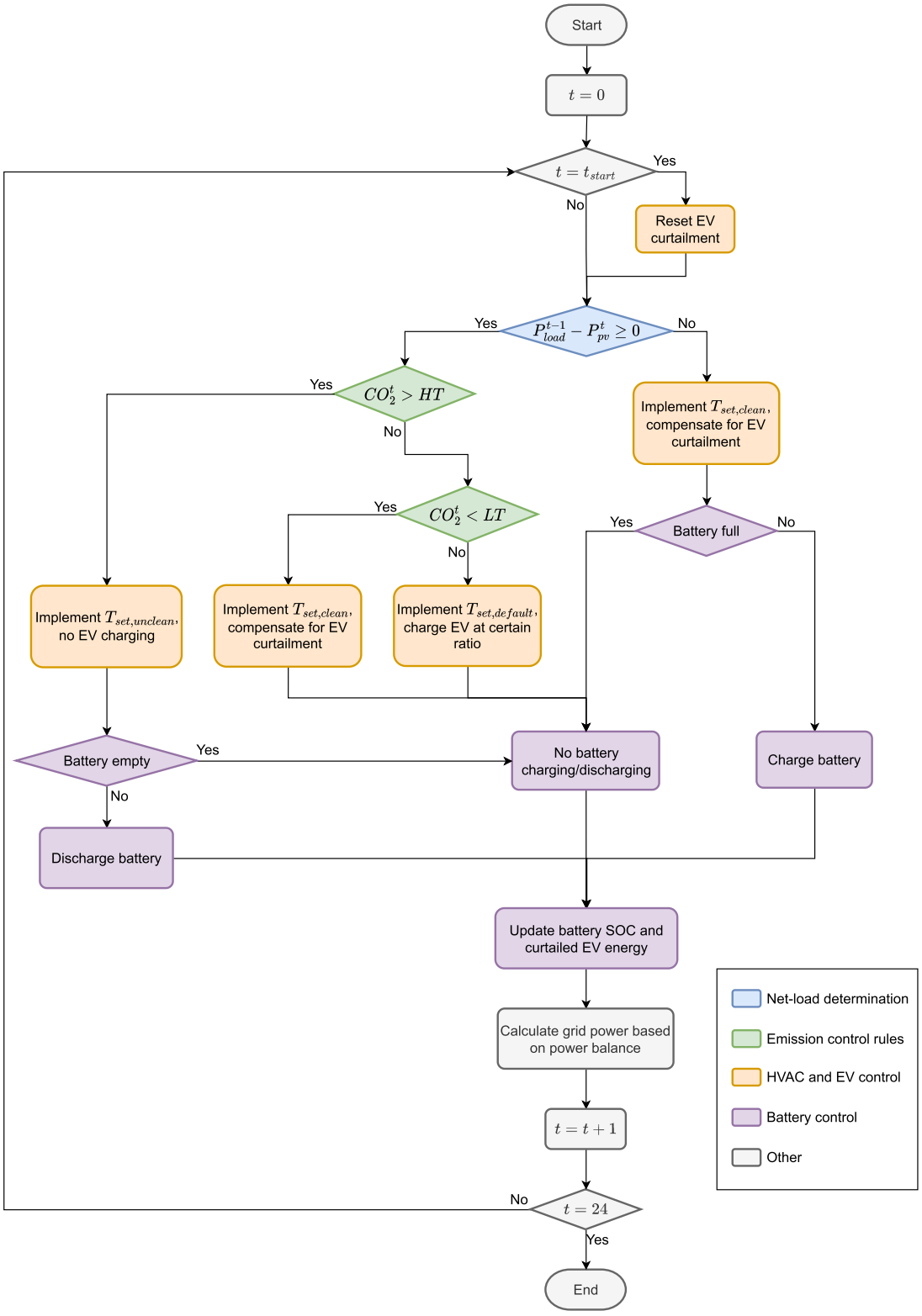

Fig. 2. The flowchart illustrates the decision-making process of the proposed coordinated control algorithm for building HVAC systems, EV charging, and battery charging/discharging based on grid carbon intensities and local PV generation. The process includes net-load determination, emission reduction control rules, HVAC and EV control, battery control, and grid power calculation.

At the end of each timestep, the total curtailed EV energy is updated with the following equation:

$$E_{curt}^{t+1} = E_{curt}^{t} + P_{curt}^{t} * \Delta t. \tag{3}$$

Considering the fact that the EVs parked at the same building change each day, we need to evaluate the EV charging control performance on a daily basis. Therefore, at the starting operational hour t_{start} of the building each day, the total curtailed EV energy of the day before will be reset to zero. Further, the EV battery state of charge (SOC) at "the end of the day" will be evaluated at one timestep before t_{start}.

Battery control The battery will only be charged when there is surplus PV generation and the battery is not full. The battery charging power is constrained by the following equation:

$$P_{bat}^{t} = \min(P_{pv}^{t} - P_{load}^{t}, P_{bat}^{\max}, E_{bat}^{\max}(1 - SOC_{bat}^{t})), \tag{4}$$

where $P_{bat}^{\max}$ is the maximum battery charging power limit; $E_{bat}^{\max}$ is the battery energy capacity; and SOC_{bat}^{t} is the current battery SOC. The building load at the current timestep P_{load}^{t} is used because battery power is calculated after the controllable loads are determined. The battery discharging only happens when the grid carbon intensity is higher than HT. In this case, the battery power will be used before the grid power kicks in. The battery discharging power is constrained by the following equation:

$$P_{bat}^{t} = -\min(P_{load}^{t} - P_{pv}^{t}, P_{bat}^{\max}, E_{bat}^{\max}(SOC_{bat}^{t} - SOC_{bat}^{\min})), \tag{5}$$

where $SOC_{bat}^{\min}$ is the minimum allowed battery SOC. After the battery power is determined at each timestep, the battery energy is then updated with the following equation:

$$E_{bat}^{t+1} = E_{bat}^{t} + P_{bat}^{t}\Delta t. \tag{6}$$

Grid power calculation Finally, the electric power draw from the grid is calculated with the following power balance equation:

$$P_{grid}^{t} = P_{load}^{t} + P_{bat}^{t} - P_{pv}^{t}, \tag{7}$$

where a positive value indicates using electricity from the grid, and a negative value indicates the backfeeding of electricity.

2.2. Baseline control

The baseline control does not include any carbon reduction algorithms. Instead, for the HVAC system, the default heating and cooling thermostat setpoints are used. The EV loads adopt the original pre-generated load profiles as previously mentioned. The battery control uses a default electricity price-driven control logic shown in Fig. 3. Similar to the coordinated control, this flowchart repeats everyday for the baseline scenario.

At the beginning of each timestep, the net-load of the building $(P_{load}^{t} - P_{pv}^{t})$ needs to be calculated. Because the total building load will be known before the battery power post-processing, the building load P_{load}^{t} will be used for the net-load calculation. Similar to the coordinated control, the battery will only be charged when the net-load is negative and the battery is not full. A mathematical description of this logic is shown in Eq. (4). Given that the utility rate structure will have peak demand charges, which typically make up a significant portion of energy bills, the battery discharging should help mitigate the peak building loads and thus reduce total energy bills. Therefore, the battery in the baseline scenario only discharges when it is the peak hour for residential buildings or peak month (i.e., months with a higher demand charge) for commercial buildings. The same mathematical description for battery discharging shown in Eq. (5) can be applied here. At the end of the timestep, the grid power will be calculated through the power balance in Eq. (7). The battery SOC will be updated with Eq. (6).

2.3. Evaluation metrics

The performance of the emission reduction control is evaluated from multiple perspectives. First, annual operational carbon emissions from the total building loads, as well as those from the HVAC system and EVs, are compared between the controlled scenario and the baseline. The following equation calculates the annual operational emissions:

$$C = \sum_{t=1}^{N} e_{\mathrm{CO_2}}^{t} P_{grid}^{t} \Delta t, \tag{8}$$

where N is the total number of simulation timesteps in a year, and $e_{\mathrm{CO_2}}^{t}$ represents the marginal carbon intensity of the grid power generation mix at each timestep. Carbon net-metering is considered in the calculation, meaning that the PV energy exported back to the grid brings in both renewable credits and carbon emissions offsetting benefits.

The annual energy consumption and cost are calculated to facilitate the analysis. Because energy net-metering is considered, both the gross annual building energy consumption and the net energy consumption are evaluated. Eq. (9) defines the annual net energy consumption:

$$E_{net} = \sum_{t=1}^{N} (P_{load}^{t} - P_{pv}^{t})\,\Delta t, \tag{9}$$

where P_{load}^{t} is the total building power demand at each timestep t, and P_{pv}^{t} is the PV generation at each timestep. Similar to the operational emissions calculation, the energy cost is obtained by multiplying the hourly grid power with the corresponding time-of-use rate. The detailed utility rate structure is introduced in Section 3.

The grid impact of the control is evaluated with the monthly peak demand as power distribution system planning is mainly dependent on the regional peak demand. The impact on occupant thermal comfort is quantified by the predicted mean vote (PMV) values of the building thermal zones. According to ASHRAE Standard 55 [22], it is calculated based on the measured air velocity, air temperature, mean radiant temperature, relative humidity, and the expected clothing level and metabolism rate of the occupants. The calculated PMV values in the OpenStudio building models for each thermal zone are averaged for the whole building evaluation.

Finally, selected DER performances are compared between the controlled and baseline scenarios. The EV battery SOC is calculated to see how much the emission reduction control affects EV drivers' need for a full battery at the end of the day. Because no arrival or departure events are modeled in this work, the EV battery SOC at the timestep before t_{start} in Fig. 2 is used instead. The PV self-consumption rate (SC) is expressed with the following equation:

$$SC_{pv} = 1 - \frac{\sum_{t=1}^{N} P_{back}^{t}\,\Delta t}{\sum_{t=1}^{N} P_{pv}^{t}\,\Delta t}, \tag{10}$$

where P_{back}^{t} is the backfeeding PV power, and P_{pv}^{t} is the total generated PV power.

3. Case study

The performance of the proposed control algorithm is validated on a model of a mixed-use community under construction in Denver, Colorado, United States. The region has a cold and dry climate and is classified as climate zone 5B according to ASHRAE Standard 169 [23]. The planned community will have 148 buildings, most of which are large commercial buildings. Figure 4 visualizes the community with color-coded building types. The detailed building types include: 36 multifamily, 23 office, 19 retail with food service, 15 office with retail, 14 strip shopping mall, 12 stand-alone retail, 6 outpatient health care, 4 large hotel, and 3 middle school. The floor areas of those buildings range from 222 to 47,283 square meters.

The community is designed to be all-electric except some natural gas usage in food service buildings for cooking. In terms of the HVAC system type, air-source heat pumps are used in residential buildings. Packaged rooftop heat pumps, packaged variable air volume (VAV) with parallel fan-powered (PFP) boxes, or VAV chiller with PFP boxes are used in commercial buildings depending on the number of floors and

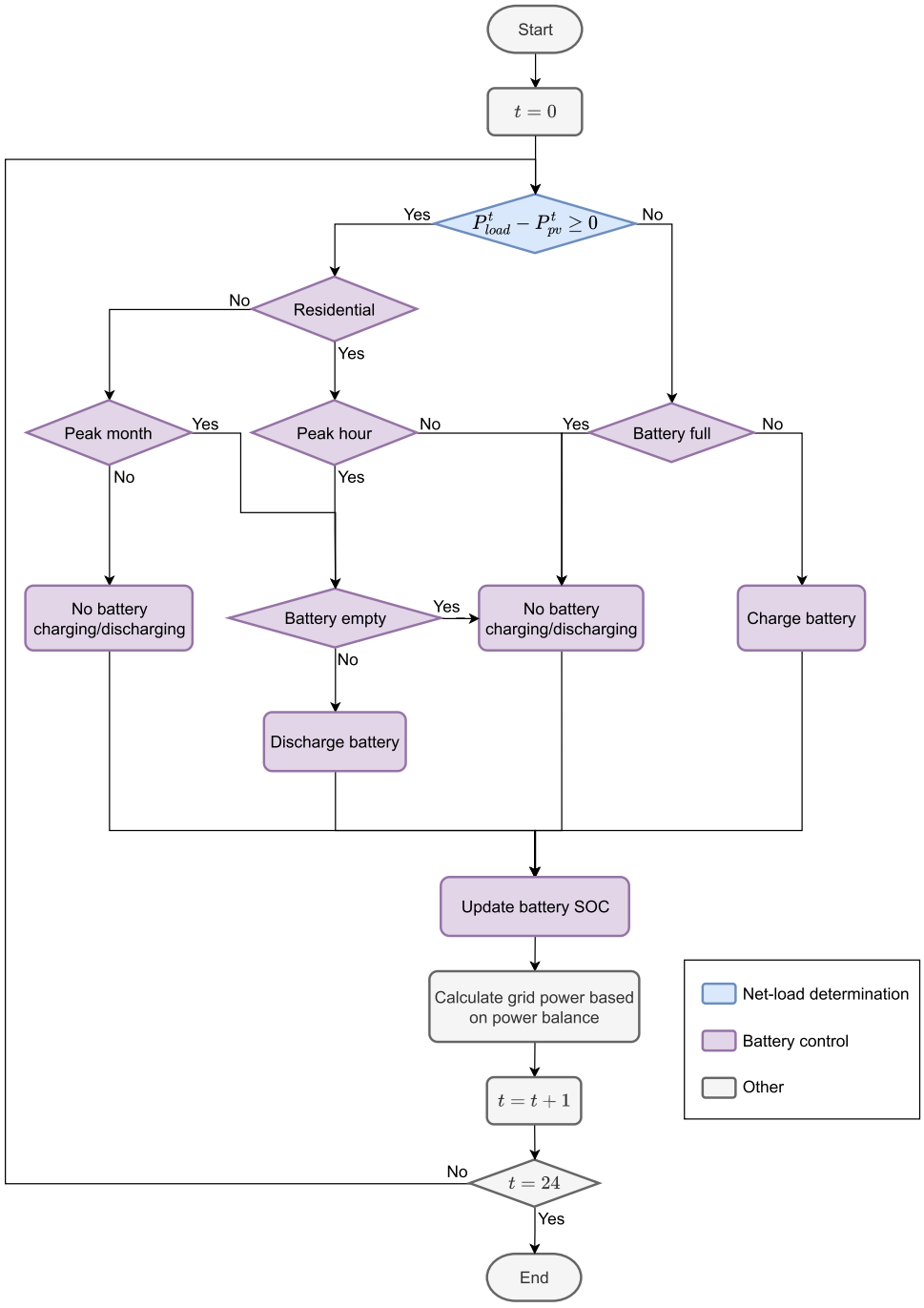

Fig. 3. The default electricity price-driven control logic used for battery control in the baseline scenario. It calculates the net-load of the building at the beginning of each timestep to ensure the battery only charges with local PV energy. The battery only discharges during peak building loads to help reduce total energy bills.

floor area [24]. The water heating systems are also electric. In food service buildings (i.e., restaurants), some natural gas usage remains for the natural gas-fueled cooking equipment, which aligns with Denver's Net Zero Energy (NZE) implementation plan [2]. The natural gas use is small compared to the electric loads and thus not included in the NZE calculations.

Electricity rates from local utility company Xcel Energy [25] are used to calculate the energy costs and implement the battery control in the baseline. Table 2 shows the rate structure for residential and commercial buildings separately [26,27]. The renewable energy credit (REC) represents the payment from utilities for the surplus PV generation in customer premises.

The grid carbon intensity data from the Cambium data set [28] are used in our case study. Cambium is based on modeled future scenarios of the U.S. electricity sector and provides forecast of future grid carbon intensities through 2050. More specifically, the 2022 hourly short-run marginal carbon emission data from the Cambium 2021 Mid-case 95 by 2035 scenario for Denver's local balancing authority is used in our analysis. This scenario assumes the CO_2 emissions in the U.S. power sector decrease to 95% below 2005 levels by 2035 and are net zero by 2050. The carbon intensity profile used in this work ranges from 0 to 2991.7 kg/MWh, with a mean value of 983.5 kg/MWh. Figure A.1 plots the 2022 annual grid carbon intensity profile. Under the same scenario, the maximum carbon intensity drops to 948.0 kg/MWh, and the mean value drops to 278.8 kg/MWh for 2050.

Typical meteorological year 3 (TMY3) data for the weather station near Denver International Airport are used as the simulation weather data. As mentioned above, EV charging load profiles are

Table 2
Local electric utility rates for residential and commercial customers, including fixed charge, energy charge, and demand charge. Energy net-metering is enabled. Table was first used in Wang et al. [20].

Item	Residential rate	Commercial rate
Fixed charge ($/month)	5.58	39.3
Energy charge ($/kWh)	0.03035 (off-peak); 0.04631 (on-peak)	0.040246
Demand charge ($/kW)	12.33 (Oct.–May); 15.54 (Jun.–Sep.)	18.45 (Oct.–May); 22.47 (Jun.–Sep.)
Net-metering	Yes	Yes
REC payment ($/kWh)	0.005	
Excess PV payment ($/kWh)	0.011	

Fig. 4. Three-dimensional rendering map of the mixed-use case study community located in Denver, Colorado, United States. The community is planned to have 148 buildings, most of which are large commercial buildings. Figure was first used in Wang et al. [20].

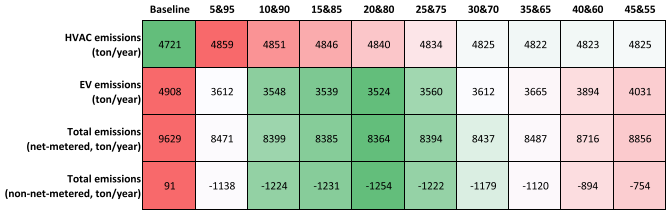

	Baseline	5&95	10&90	15&85	20&80	25&75	30&70	35&65	40&60	45&55
HVAC emissions (ton/year)	4721	4859	4851	4846	4840	4834	4825	4822	4823	4825
EV emissions (ton/year)	4908	3612	3548	3539	3524	3560	3612	3665	3894	4031
Total emissions (net-metered, ton/year)	9629	8471	8399	8385	8364	8394	8437	8487	8716	8856
Total emissions (non-net-metered, ton/year)	91	-1138	-1224	-1231	-1254	-1222	-1179	-1120	-894	-754

Fig. 5. The results of the sensitivity analysis, comparing the annual carbon emissions of nine combinations of low and high thresholds for the proposed coordinated control algorithm. The greener the color, the lower the emissions are. The plot reveals that the combinations of 10&90 to 30&70 perform similarly, with the combination of 20&80 outperforming the others in terms of EV and whole building total emissions.

pre-generated by EVI-Pro and then input into the simulation framework. Figure A.2 plots the EV charging profiles for one selected building in each building type of the community. Annual energy simulations with an hourly timestep for 2022 was conducted for two scenarios: baseline scenario and controlled scenario. The baseline scenario is designed to be NZE on an annual basis.

4. Results and discussion

This section first presents the sensitivity analysis results to justify the control threshold selection in this paper. Then, we discuss the performance of the proposed emission reduction control algorithm in terms of its annual emission reduction potential and the underlying energy consumption changes. Its impact on building energy costs, peak demand, and thermal comfort will then be evaluated. Finally, the DER performances such as the EV battery SOC and PV self-consumption rate are compared between the baseline and the controlled scenario.

4.1. Sensitivity analysis

The control rules in rule-based controllers need to be carefully designed to yield the best control results. For the proposed emission reduction controller in this work, the rule design is essentially to choose the control threshold values of the HT and LT. More specifically, the values are selected based on the grid carbon intensity input data. Because the distributions and ranges of the input data vary, percentiles are used to define the thresholds.

As shown in Fig. 5, nine evenly distributed combinations of HTs and LTs were investigated and the annual carbon emission results are compared with the baseline. The sensitivity analysis was conducted using ten sample buildings (one from each type) randomly selected from the community to save computational effort. In the plot, the greener the color, the lower the emissions are. From the figure, the performance of the combinations from 10&90 to 30&70 do not change drastically, while the remaining combinations perform noticeably worse. Looking at the detailed annual carbon emissions data, the HVAC system emissions, excluding the baseline, are lowest when using the combination of 35&65. For the EV and whole building total emissions, the combination of 20&80 outperforms the others. Therefore, we chose to implement the LT of the 20th percentile with the HT of the 80th percentile of the carbon intensity data in the proposed rule-based controller. Note that this rule design is dependent on the input carbon data distribution along with the building load profiles, and is thus not applicable to all cases. However, the methodology for conducting the sensitivity analysis can be adopted by similar studies.

4.2. Annual carbon emissions

The whole building annual emissions show significant decreases ranging from 4.5% to 27.1% across different buildings, which is primarily attributed to the 10.9%–32.7% EV emission reduction. Figure 6 shows the distribution of building annual total emissions, net emissions, and the emissions from the HVAC systems and EVs through violin plots. Each point in the plots represents the annual emissions of one building. In the upper left plot, more buildings are distributed in the lower half of the violin for the controlled scenario and the maximum emissions value drops from over 7000 tons/year to over 6000 tons/year. More drastically, in the upper right plot where carbon net-metering is considered, a long tail of the violin for the controlled scenario is seen. This is caused by more PV backfeeding into the grid, which considerably offsets the annual carbon emissions in some buildings. Comparing the emissions from the controlled loads, we see more prominent emission reductions in the EVs than the HVAC systems, potentially due to the HVAC energy increases explained in the following paragraph. Overall, the application of the proposed emission reduction control algorithm has led to a significant whole building emission reduction. The directly controllable loads (i.e., EVs) perform better than thermostatically controllable loads (TCLs) (i.e., HVAC system). The emission reduction from TCLs can be enhanced by adding thermal energy storage, which will be a topic for our follow-on work.

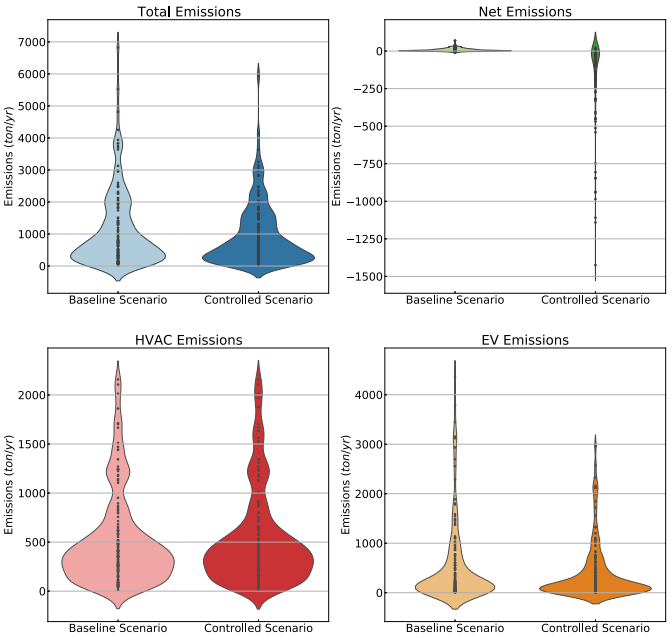

Fig. 6. Violin plots of the distribution of building annual total emissions, net emissions, and emissions from HVAC systems and EVs. Each point in the plots represents the annual emissions of one building. The application of the proposed emission reduction control algorithm has led to a significant whole building emission reduction, with more prominent emission reductions in the EVs than the HVAC systems.

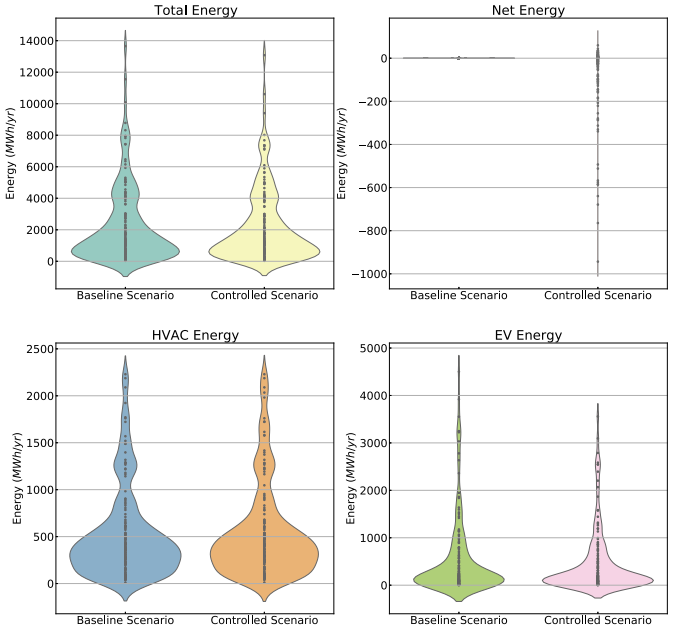

Fig. 7. Violin plots of the distribution of building annual energy consumption, including total, net, EV, and HVAC energy. The figure highlights that shifting loads to lower carbon intensity hours can lead to effective emission reductions, which further indicates that not only the total energy consumption matters but also when it is consumed.

The analysis of the annual energy results in Fig. 7 proves that not only does the total energy consumption matter, but also when it is consumed matters. From the figure, we notice very similar distributions between the emissions and energy. Further, the NZE design of the baseline scenario makes its distribution violin a horizontal line in the upper right plot. On average, there are 1.0% total energy reductions with 11.9% EV energy reductions. The HVAC energy increases by 5.0% on average, potentially because of the emission reduction-driven objective of the control algorithm and the standby heat losses of TCLs. Similar findings are discussed in Wang et al. [10]. However, for any of the load types, the proportions of the energy changes are smaller than those of their emission changes. This showcases that the shifting of the loads toward lower carbon intensity hours can effectively bring about emission reductions, as when the energy is consumed matters.

4.3. Impact of the coordinated control

4.3.1. Energy costs

The annual total energy cost remains almost the same with a slight decrease of 0.7% after the application of the controller. This suggests that no roadblock for the adoption of the proposed controller will arise from an economic perspective. From Fig. 8, we see a larger change in the energy charge than in the demand charge and PV credit. More specifically, the annual average energy charge is reduced by 7.5% on average, which is more significant than the annual total energy reduction of 1.0%. This indicates that there are more peak hour energy consumption reductions than off-peak hours. This is attributable to the general alignment between peak hours and high carbon intensities of the grid. The average demand charge increases moderately by 1.2%; this can be explained by the peak demand increases discussed in the following subsection. The average PV credit decreases by 2.7%, which implies more PV self-consumption induced by the control algorithm. More details about the PV self-consumption rate will be discussed in Section 4.4.2. It is noted that although more backfeeding is seen in the controlled scenario, the PV credit is mostly affected by the REC payment in Table 2 and the

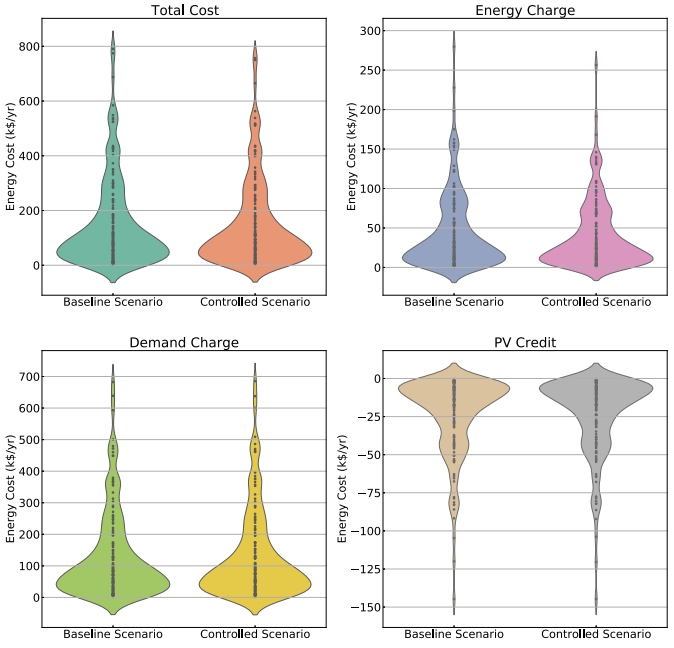

Fig. 8. Violin plots of annual total energy costs and contributing components including the energy charge, demand charge, and PV credit. The energy charge shows a larger reduction than the demand charge and PV credit, with an average reduction of 7.5%. The total energy cost decreases by 0.7%, suggesting that the proposed controller is economically feasible.

excess PV payment only accounts for a small portion. Therefore, the lower right plot of Fig. 8 shows a similar distribution between the two scenarios.

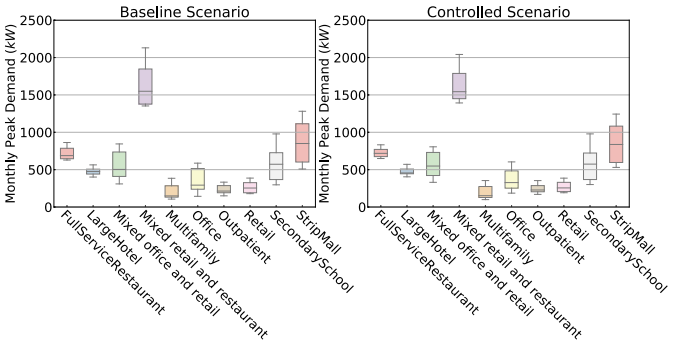

Fig. 9. Boxplots of monthly peak demand by building type. Each point in the boxes represents the average peak demand value of one month from the corresponding building type. The figure indicates that the emission reduction-driven battery control performs less satisfactorily than the price-driven control in lowering peak demands and demand charges.

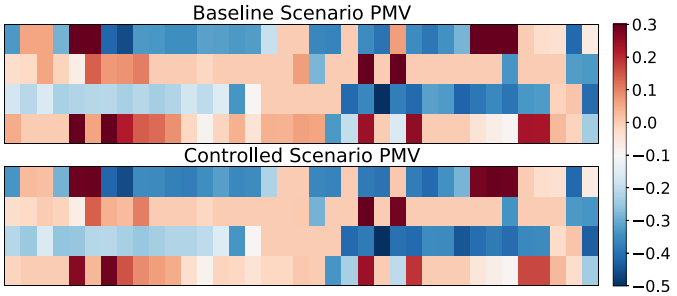

Fig. 10. Color plots of annual average zone mean PMV values per building before and after the implementation of the emission reduction control. Each color block represents one building. The emission reduction control has slightly lowered the community average PMV value by 0.02, indicating a slightly colder indoor environment, but the adoption of the control will not impact the occupants' thermal comfort with the design parameters proposed in this work.

4.3.2. Peak demand

The community-level average monthly peak demand values reflect the impact of the different battery control strategies in the baseline and the controlled scenario. Figure 9 is the boxplot of monthly peak demand by building type. Each point in the boxes represents the average peak demand value for one month within the corresponding building type. From the figure, we see both peak demand increases and decreases across building types with no explicit trend. By analyzing the data, we notice an overall trend of peak demand decrease in winter and increase in summer. This can be attributed to the fact that the price-driven battery control in the baseline scenario helps reduce the peak demand in the peak season (i.e., June–September) effectively. However, the emission reduction-driven battery control only discharges the battery when the grid intensity is high, which happens less frequently in summer due to the high PV generation in summer. The seasonal variations of peak demands also lead to the rise of demand charges in the controlled scenario as the utility summer demand charge is higher than winter. To summarize, the emission-driven battery control performs less satisfactorily than the price-driven control in lowering peak demands and demand charges.

4.3.3. Thermal comfort

There are negligible changes to the thermal comfort of the building occupants after the implementation of the emission reduction control. As mentioned above, the thermal comfort is evaluated by PMV values in this work. Figure 10 plots the annual average zone mean PMV values per building for the baseline and the controlled scenario. Each color block in the plot represents one building. Given that all the PMV values lie within the range of −0.5–0.3, it is neither too hot nor too cold regardless of the control method. On average, the emission reduction control has lowered the community average PMV value by 0.02, which indicates a slightly colder indoor environment. Generally, it is safe to say that the adoption of the emission reduction control will not affect building occupants' thermal comfort with the design parameters proposed in this work.

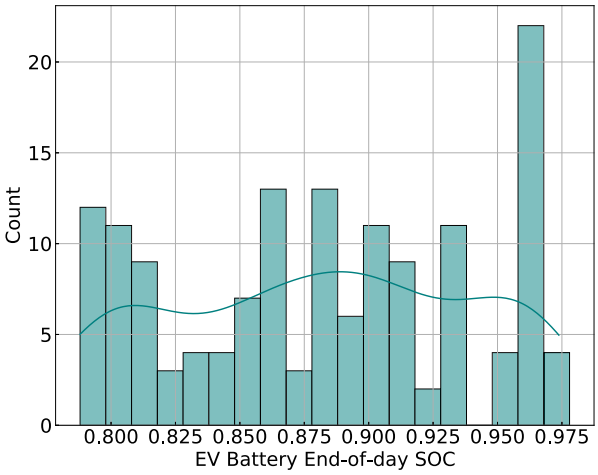

Fig. 11. Histogram of annual average EV end-of-day SOC for the coordinated control scenario. The baseline EV SOC is considered to be 1 (i.e., fully charged). The plot reveals that the EV SOC values for all buildings fall within the range of 0.790.97, with a community mean value of 0.88. The results also suggest that the emission reduction control can strike a balance between the EV range and environmental impact.

4.4. DER performances

4.4.1. EV battery SOC

A certain amount of EV battery end-of-day SOC reduction was noticed, which lies in a reasonable range. The EV SOC reduction is as expected because of the curtailment of EV charging power when the grid carbon intensity is higher than the LT. Given the limited number of clean hours throughout a day and the EV charging power upper limit, it is plausible that not all curtailed EV energy will be compensated during the same day. Figure 11 shows the histogram of the annual average EV end-of-day SOC for the controlled scenario. From the figure, the EV SOC values for all buildings lie within the range of 0.79–0.97 with a community mean value of 0.88. Considering the EV emission reduction effect, 2.6% to 21.2% of EV SOC reduction results in 10.9% to 32.7% of EV emission reductions. This result demonstrates that the emission reduction control can help achieve a balance between the EV range and the environmental impact.

4.4.2. PV self-consumption rate

The PV self-consumption rate is increased in the controlled scenario due to the higher HVAC and EV charging loads when the building net-load is negative. Based on Fig. 12, there exists an average increase of 6.0% PV self-consumption rate after the adoption of the emission reduction control. In some buildings, a decrease of up to 0.9% is seen, while in most buildings, the self-consumption rate is increased by up to 21.2%. We note that this does not conflict with the negative net emissions and energy values in Figs. 6 and 7, as the self-consumption rate is calculated in proportion to the annual total PV generation (Eq. (10)). Buildings with larger amounts of backfeeding also tend to have higher PV generation. In summary, through the emission reduction control, more clean energy is consumed locally rather than being fed back to the grid. This reduces transmission and distribution losses and supports higher PV penetration in the distribution grid.

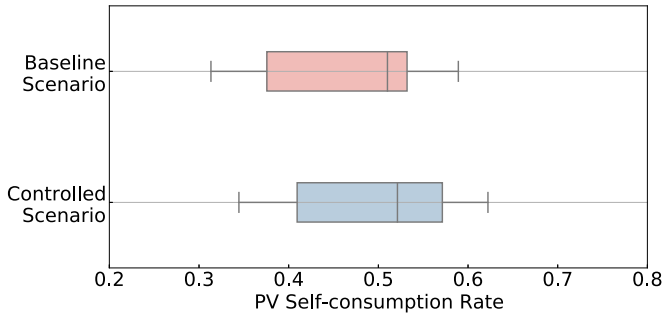

Fig. 12. Boxplots of the annual average PV self-consumption rate per building. Each point in the box represents one building. The plot shows an overall increase in PV self-consumption rate with a maximum increase of 21.2%, indicating that the emission reduction control leads to more local consumption of clean energy, supporting higher PV penetration in the distribution grid.

5. Conclusion

In this work, we propose a rule-based coordinated control of EV charging and HVAC systems for reducing carbon emissions in all-electric buildings. Local PV generation is included in the control design as one of the control inputs. Behind-the-meter batteries are involved to enhance load shifting. Grid carbon intensity data is used as the main decision variable to facilitate threshold-based load shifting to lower emission rate hours. A case study of a mixed-use community under construction in Denver, Colorado, United States, is conducted to evaluate the control performance. The goal of this research is to fill the gap of lacking easy-to-implement community-scale coordination of buildings and EVs in the current state of the art of emission reduction control.

Through analysis of the simulation results, we identified 4.5% to 27.1% of annual whole building emission decreases, where a large portion is attributed to the 10.9%–32.7% EV emission reductions. The HVAC system emission increases by 3.6% annually while its energy increase is 5.0% on average. The cross-comparison between energy and emission shows that not only does the total energy consumption matter, but also when the energy is consumed matters.

In terms of the impact of adopting the emission reduction control, the annual total energy cost remains almost the same, with a slight decrease of 0.7% after the application of the controller. The community average monthly peak demand values generally increase in summer and decrease in winter, which reflects that the emission-driven battery control performs less satisfactorily than the price-driven control in lowering peak demands and demand charges. Changes to the thermal comfort of the building occupants are negligible after the control implementation. EV battery end-of-day SOC reductions of 2.6% to 21.2% are noticed, which balance between the EV range and the environmental impact of EV charging. The PV self-consumption rate is increased in the controlled scenario due to the higher HVAC and EV charging loads when the building net-load is negative.

The limitation of this work is not including more controllable loads and DERs into the control framework. Further, the control only targets one objective of emission reductions, with limited consideration of lowering peak demands. This is also a common limitation of general rule-based controllers. Lastly, perfect forecasts of the grid carbon emission intensity data are assumed. Future work will involve addressing the noted limitations, such as the integration of thermal energy storage.

Declaration of Competing Interest

The authors declare that they have no known competing financial interests or personal relationships that could have appeared to influence the work reported in this paper.

Data availability

The authors do not have permission to share data.

Acknowledgments

This work was authored by the National Renewable Energy Laboratory, operated by Alliance for Sustainable Energy, LLC, for the U.S. Department of Energy (DOE) under Contract No. DE-AC36-08GO28308. Funding provided by NREL's Laboratory Directed Research and Development program. The views expressed in the article do not necessarily represent the views of the DOE or the U.S. Government. The U.S. Government retains and the publisher, by accepting the article for publication, acknowledges that the U.S. Government retains a nonexclusive, paid-up, irrevocable, worldwide license to publish or reproduce the published form of this work, or allow others to do so, for U.S. Government purposes.

Appendix A

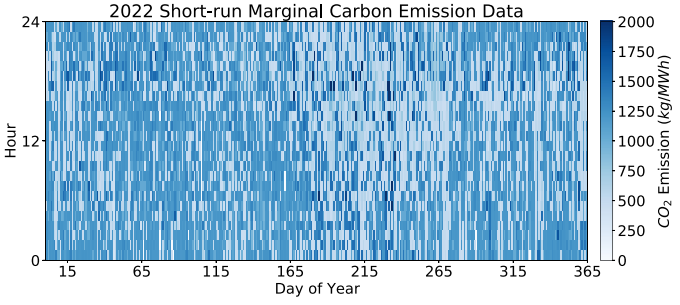

Fig. A.1. The 2022 annual grid carbon intensity profile used in the study, ranging from 0 to 2991.7 kg/MWh, with a mean value of 983.5 kg/MWh. The maximum carbon intensity drops to 948.0 kg/MWh, and the mean value drops to 278.8 kg/MWh for 2050 under the same scenario.

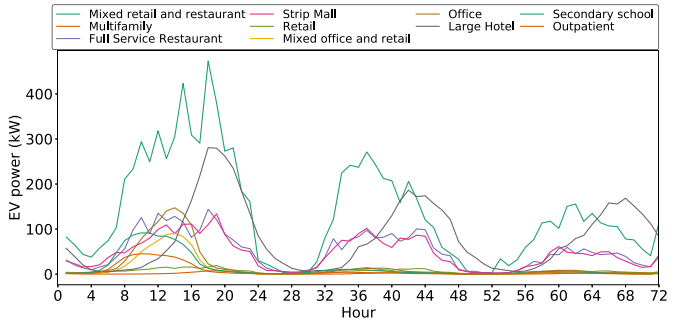

Fig. A.2. EV profiles for one building of each building type of the community on three summer days (one weekday and two weekends). The *x*-axis represents the time in hour, and the *y*-axis represents the power (kW) of the EV charger. It can be seen that after a buildings normal operation hours, much less EV charging power occur.

References

[1] U.S. Energy Information Administration. What are U.S. energy-related carbon dioxide emissions by source and sector?2022. Accessed 19 September 2022 https://www.eia.gov/tools/faqs/faq.php?id=75&t=11.

[2] . Denver's net zero energy (NZE) new buildings & homes implementation planTech. Rep.. Denver Climate Action, Sustainability & Resiliency Office and New Buildings Institute; 2021.

[3] International Energy Agency. Global electric car sales have continued their strong growth in 2022 after breaking records last year. 2022. Accessed 19 September 2022; https://www.iea.org/news/global-electric-car-sales-have-continued-their-strong-growth-in-2022-after-breaking-records-last-year.

[4] Leerbeck K, Bacher P, Junker RG, Tveit A, Corradi O, Madsen H, Ebrahimy R. Control of heat pumps with CO_2 emission intensity forecasts. Energies 2020;13(11):2851.

[5] Gasser J, Cai H, Karagiannopoulos S, Heer P, Hug G. Predictive energy management of residential buildings while self-reporting flexibility envelope. Appl Energy 2021;288:116653.

[6] Dixon J, Bukhsh W, Edmunds C, Bell K. Scheduling electric vehicle charging to minimise carbon emissions and wind curtailment. Renew Energy 2020;161:1072–91.

[7] Jeen S.R., Abate A., Cullen J.M.. Low emission building control with zero-shot reinforcement learning. arXiv preprint arXiv:220806385 2022.

[8] Fischer D, Madani H. On heat pumps in smart grids: a review. Renew Sustain Energy Rev 2017;70:342–57. doi:10.1016/j.rser.2016.11.182.

[9] Clauß J, Stinner S, Sartori I, Georges L. Predictive rule-based control to activate the energy flexibility of Norwegian residential buildings: case of an air-source heat pump and direct electric heating. Appl Energy 2019;237:500–18.

[10] Wang J, Munankarmi P, Maguire J, Shi C, Zuo W, Roberts D, et al. Carbon emission responsive building control: a case study with an all-electric residential community in a cold climate. Appl Energy 2022;314:118910.

[11] Wang J, El Kontar R, Jin X, King J. Feasibility study of real-time carbon emission responsive electric vehicle charging control in buildings. ACEEE 2022 summer study on energy efficiency in buildings. ACEEE; 2012.

[12] Péan T, Costa-Castelló R, Salom J. Price and carbon-based energy flexibility of residential heating and cooling loads using model predictive control. Sustain Cities Soc 2019;50:101579.

[13] Shi W, Karimzadeh M. Automating load shaping for EVs: optimizing for cost, grid constraints, andQ carbon?. Tech. Rep.. Sense Labs and Singularity Energy; 2021.

[14] Tu R, Gai YJ, Farooq B, Posen D, Hatzopoulou M. Electric vehicle charging optimization to minimize marginal greenhouse gas emissions from power generation. Appl Energy 2020;277:115517.

[15] Polly B, Kutscher C, Macumber D, Schott M, Pless S, Livingood B, Van Geet O. From zero energy buildings to zero energy districts. In: Proceedings of the 2016 American council for an energy efficient economy summer study on energy efficiency in buildings, Pacific Grove, CA, USA; 2016. p. 21–6.

[16] El Kontar R, Polly B, Charan T, Fleming K, Moore N, Long N, Goldwasser D. URBANopt: an open-source software development kit for community and urban district energy modeling. In: ASHRAE topical conference proceedings. American Society of Heating, Refrigeration and Air Conditioning Engineers, Inc.; 2020. p. 293–301.

[17] The American Society of Heating, Refrigerating and Air-Conditioning Engineers. ASHRAE standard 90.1-2009: Energy standard for buildings except low-rise residential buildings. 2009.

[18] National Renewable Energy Laboratory. EVI-Pro: Electric Vehicle Infrastructure Projection Tool. 2022. Accessed 23 September 2022; https://www.nrel.gov/transportation/evi-pro.html.

[19] Pless S, Allen A, Goldwasser D, Myers L, Polly B, Frank S, Meintz A. Integrating electric vehicle charging infrastructure into commercial buildings and mixed-use communities: design, modeling, and control optimization opportunities. Tech. Rep.. National Renewable Energy Laboratory, Golden, United States; 2020.

[20] Wang J, El Kontar R, Jin X, King J. Electrifying high-efficiency future communities: impact on energy, emissions, and grid. Adv Appl Energy 2022;6:100095.

[21] Cutler D, Olis D, Elgqvist E, Li X, Laws N, DiOrio N, Walker A, Anderson K. REopt: a platform for energy system integration and optimization. Tech. Rep.. National Renewable Energy Laboratory; 2021.

[22] The American Society of Heating, Refrigerating and Air-Conditioning Engineers. ASHRAE Standard 55 - Thermal Environmental Conditions for Human Occupancy. 2020.

[23] The American Society of Heating, Refrigerating and Air-Conditioning Engineers. ASHRAE Standard 169 - Climatic Data for Building Design Standards. 2021.

[24] The American Society of Heating, Refrigerating and Air-Conditioning Engineers. ASHRAE Standard 90.1-2019: Energy Standard for Buildings except Low-rise Residential Buildings, Appendix G. 2019.

[25] Xcel Energy. 2022. Accessed 11 October 2022; https://co.my.xcelenergy.com/s/.

[26] U.S. Utility Rate Database. Residential Demand - Time Differentiated Rates (Schedule RD-TDR). Accessed 27 September 2021; https://openei.org/apps/USURDB/rate/view/5ffe16745457a3817e2dfcad1_Basic_Information.

[27] U.S. Utility Rate Database. Secondary General Service (Schedule SG). Accessed 27 September 2021; https://openei.org/apps/USURDB/rate/view/60072c345457a3c14c21f941_Basic_Information.

[28] Gagnon P., Frazier W., Cole W., Schwarz M., Hale E.. Cambium data for 2021 standard scenarios. 2021. Accessed 10 October 2022; https://cambium.nrel.gov/.